Electronic Supplementary Information

Thermoresponsive Polymer Brush-Functionalized Magnetic Manganite Nanoparticles for Remotely Triggered Drug Release

Stéphanie Louguet, Bérengère Rousseau, Romain Epherre, Nicolas Guidolin, Graziella Goglio, Stéphane Mornet, Etienne Duguet, Sébastien Lecommandoux and Christophe Schatz
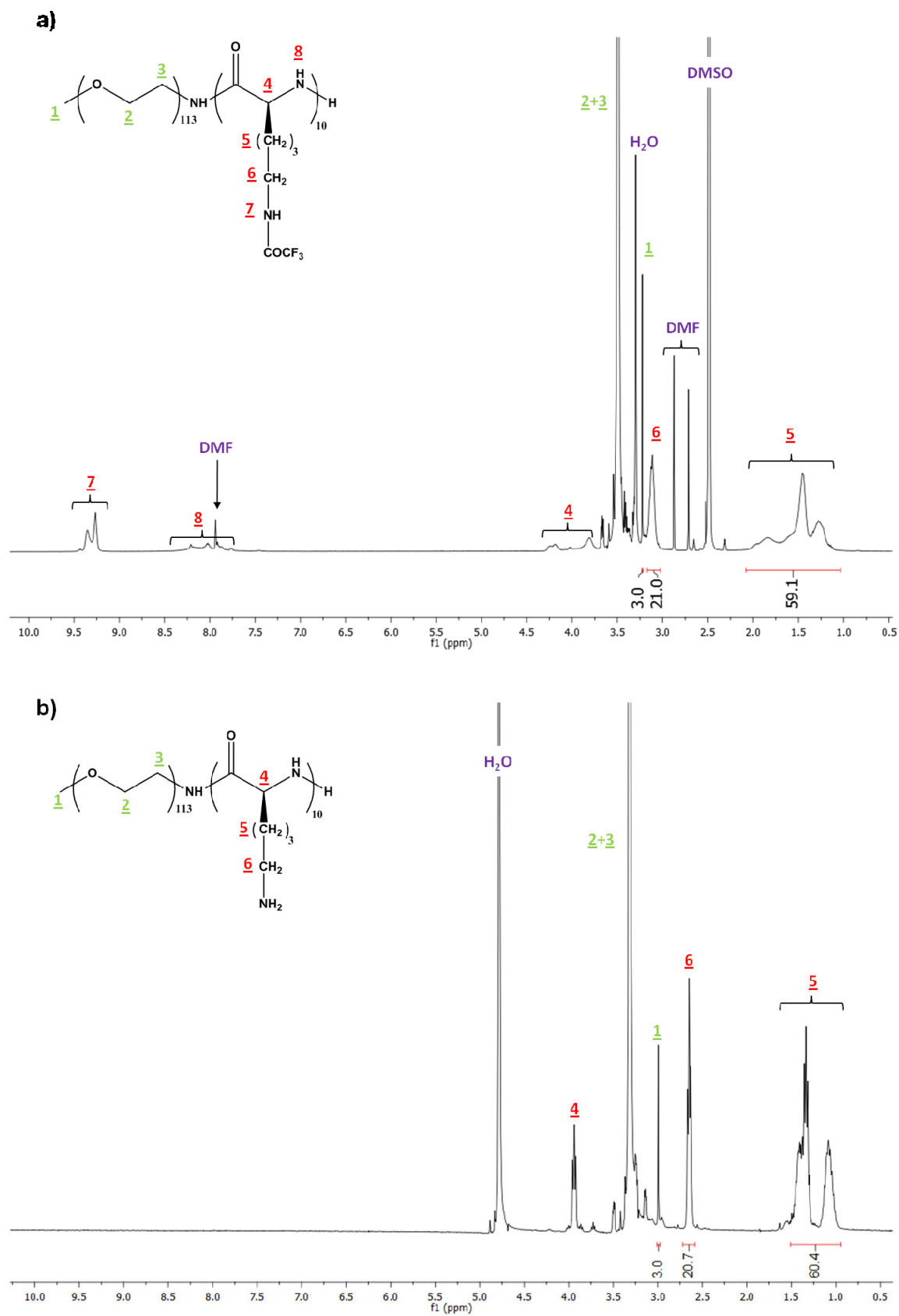
1. 1H NMR analysis of PEO-b-PLL and P(EO-co-PO)-b-PLL copolymers

^{1}H NMR spectra of PEO-*b*-PLL, P(EO$_{31}$-*co*-PO$_{10}$)-*b*-PLL and P(EO$_6$-*co*-PO$_{29}$)-*b*-PLL with TFA-protected and unprotected lysine segments are shown in Figure S1, Figure S2 and Figure S3. Protons of the unprotected amine groups were not distinguishable from the noise of the baseline as they were probably exchanged with D_2O. The degree of polymerization (DP) of the poly(TFA L-lysine) block in PEO-*b*-PTFALL was determined by comparing the peak integration of the end methyl group of PEO block (-CH$_3$, δ = 3.217 ppm) with ε-methylene protons of the lysine side chains (-CH$_2$, δ = 3.106 ppm) or with the 6 equivalent β, γ, δ-methylene protons of the lysine side chains (-(CH$_2$)$_3$, δ = 1.1 – 2 ppm). This allowed us to determine a DP of 10 for the PLL block (Figure S1a). For P(EO$_x$-*co*-PO$_y$)-*b*-PTFALL copolymers, the DP of the poly(TFA L-lysine) block was determined by considering the methyl side group as a reference (-CH$_3$, δ = 1.029 ppm). DPs of 13 and 10 were found for the PTFALL block in P(EO$_{31}$-*co*-PO$_{10}$)-*b*-PTFALL and P(EO$_6$-*co*-PO$_{29}$)-*b*-PTFALL, respectively (Figure S2a and Figure S3a). The copolymers were also characterized by ^{1}H NMR spectroscopy in D_2O with DCl (35 % w/w in D2O) after the removal of labile trifluoroacetyl (TFA) protecting groups of L-lysine. While PTFALL blocks exhibit a secondary structure (α-helix or β-sheet) through hydrogen bonding between CO and NH groups, PLL chains probably adopt a coil-like conformation after deprotection. This conformational transition was characterized by a shift of the ε-methylene protons of the lysine side chains from δ = 3.106 ppm to δ = 2.704 ppm on ^{1}H NMR spectra (Figure S1b, Figure S2b and Figure S3b). The determination of the DP of the PLL blocks after deprotection was performed by ^{1}H NMR spectroscopy using the same characteristic peaks as previously (Figure S1b, Figure S2b and Figure S3b). Results in Table S1 showed that DP values of PLL are not the same before and after deprotection, the larger difference being obtained with the copolymer having a PPO-rich polyether block. Hence, it is likely that such a difference of DP arises from the variation in solvency of the polyether blocks due to their LCST behaviour. A decrease in solubility of the polyether blocks would indeed favour an overestimation of the DP of the PLL blocks as

observed in Table S1. Therefore, the values considered in this study are the values determined from the TFA-protected form of the copolymers.

Table S1. Degrees of polymerization of PLL blocks as determined by ^{1}H NMR

|	PEO_{113}-*b*-PLL_n	$P(EO_{31}$-*co*-$PO_{10})$-*b*-PLL_n	$P(EO_6$-*co*-$PO_{29})$-*b*-PLL_n
Protected form	10	13	10
Unprotected form	10	14.5	17

**Figure S1.** ^{1}H NMR spectra of PEO-*b*-PTFALL in d$_6$-DMSO (a) and PEO-*b*-PLL in D$_2$O with DCl (b)
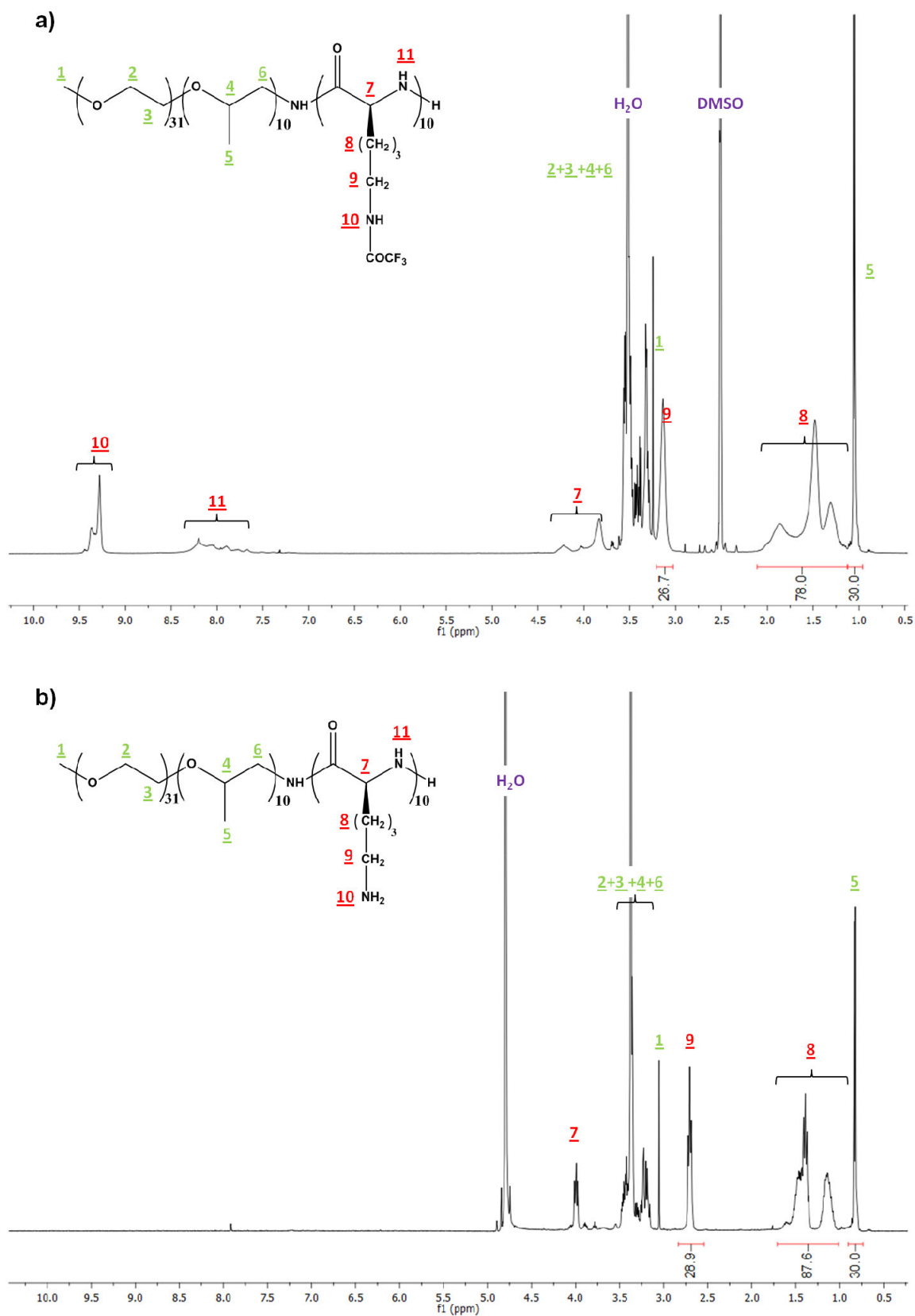
Figure S2. ^{1}H NMR spectra of P(EO$_{31}$-*co*-PO$_{10}$)-*b*-PTFALL in d$_6$-DMSO (a) and P(EO$_{31}$-*co*-PO$_{10}$)-*b*-PLL in D$_2$O with DCl (b)

a)

b)

Figure S3. ^{1}H NMR spectra of P(EO$_6$-*co*-PO$_{29}$)-*b*-PTFALL in d$_6$-DMSO (a) and P(EO$_6$-*co*-PO$_{29}$)-*b*-PLL in D$_2$O with DCl (b)
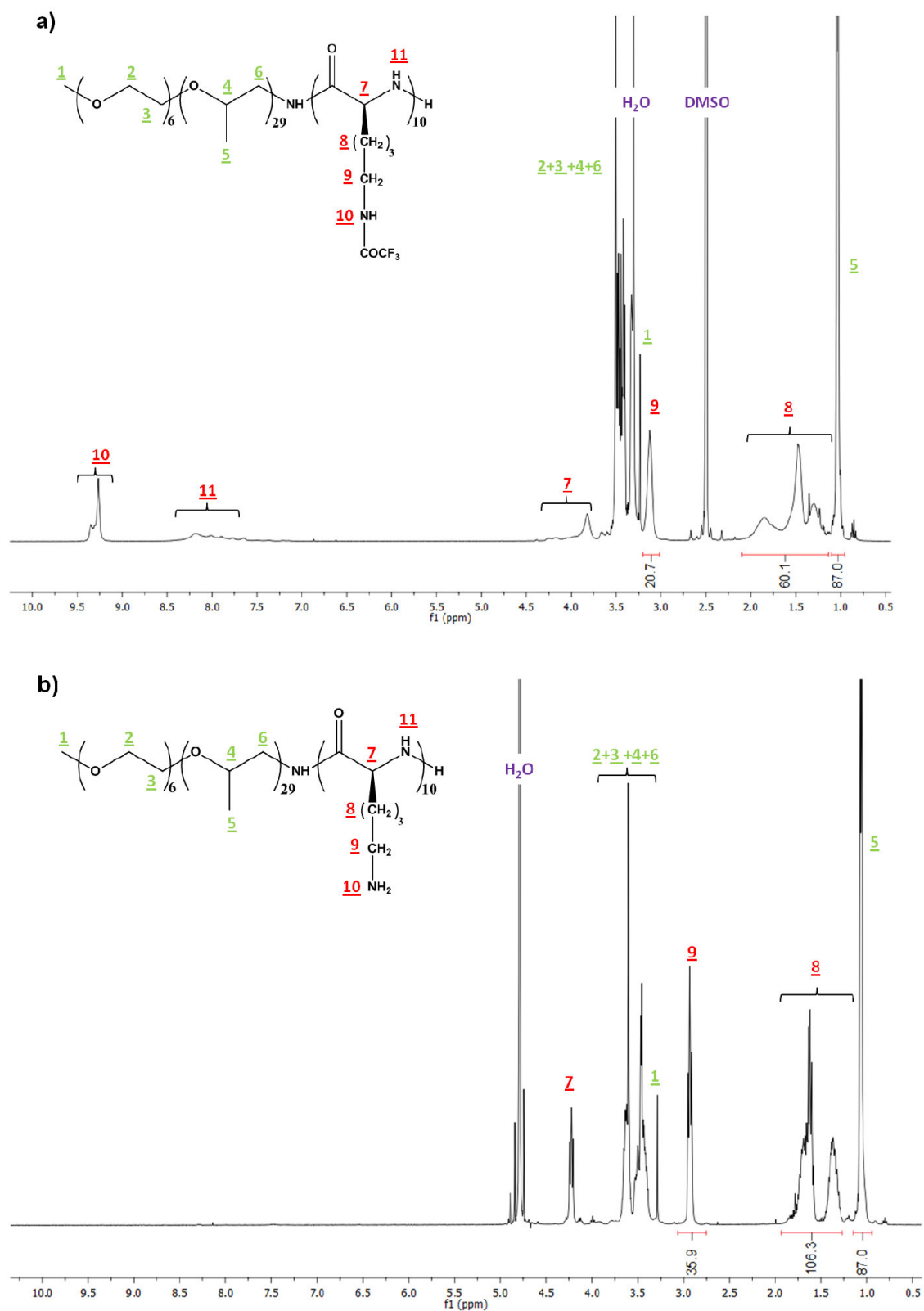
2. Conductimetric titration of the block copolymers

In addition to NMR analysis, conductimetric titrations were also performed to determine the DP of the PLL blocks (Figure S4). Block copolymers were dispersed in water with 5 mM of NaCl at c = 1 g/L and after overnight stirring the pH was adjusted below 5 by addition of a 0.1 M HCl solution. Titration experiments were carried out using a 0.1 M NaOH standard solution and an equilibration time of 4 min was applied after each addition of NaOH. The parts 1, 2 and 3 in the conductimetric profiles refer to the titration of excess HCl, of lysine residues and of excess NaOH, respectively.
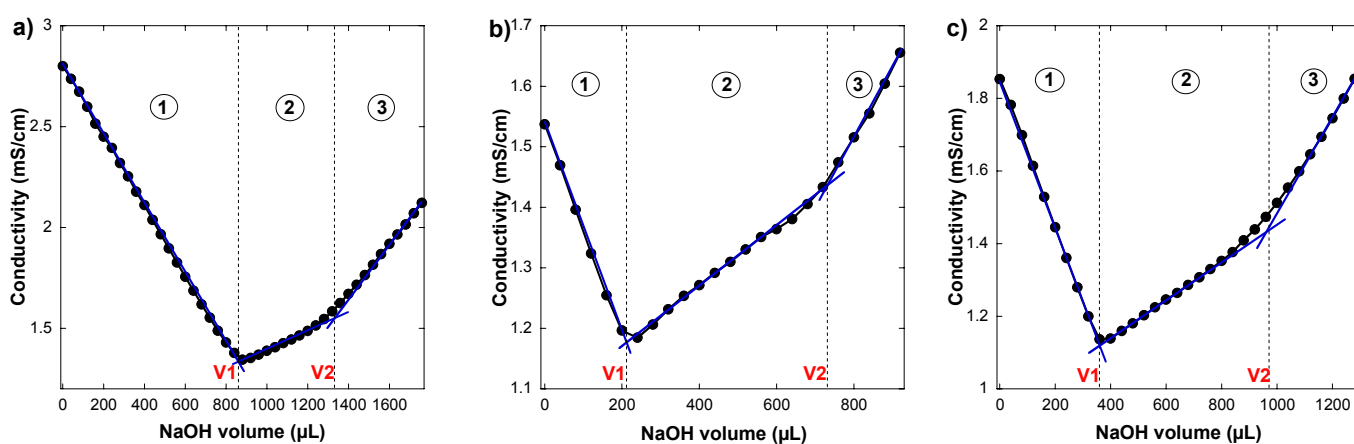
Figure S4. Conductimetric titration of PEO$_{113}$-*b*-PLL (a), P(EO$_{31}$-*co*-PO$_{10}$)-*b*-PLL (b) and P(EO$_6$-*co*-PO$_{29}$)-*b*-PLL (c) .

DP of PLL blocks were calculated from conductimetric plots using the following equation:

$$\overline{DP}(PLL) = \frac{n_{OH^-} \times M_{Polyether}}{\left(m_{BCP} - M_{LL} \times n_{OH^-}\right)}$$

where m_{BCP} refers to the mass of block copolymer, $M_{Polyether}$ and M_{LL} to the molar mass of polyether blocks and lysine units (129 g/mol) and n$_{OH^-}$ to the amount of added NaOH. Results are gathered in Table S2.

Table S2. Degree of polymerization of PLL blocks as determined by conductimetric titration.

	m_{BCP} mg	Titration start μL	Titration end μL	n
PEO$_{113}$-b-PLL$_n$	31	870	1350	9.6
P(EO$_{31}$-co-PO$_{10}$)-b-PLL$_n$	15	210	760	12.8
P(EO$_6$-co-PO$_{29}$)-b-PLL$_n$	20	360	980	10.2

3. LCST of polyether blocks.

The critical solution temperatures of P(EO$_6$-co-PO$_{29}$) and P(EO$_{31}$-co-PO$_{10}$) polyethers were determined by light scattering measurements. Both polyethers were solubilized in water at c = 10 g/L and the variation of scattering intensities were recorded with increasing temperatures (Figure S5). Critical temperatures of 35 °C and 16 °C were respectively determined for P(EO$_{31}$-co-PO$_{10}$) and P(EO$_6$-co-PO$_{29}$).
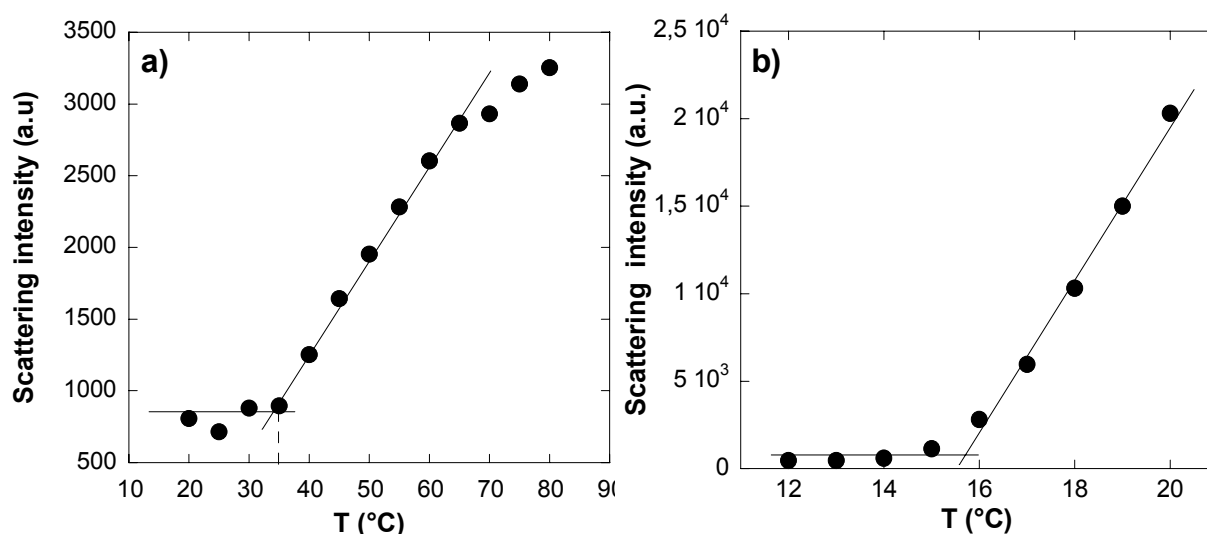

Figure S5. Scattering intensities of P(EO$_{31}$-co-PO$_{10}$) (a) and P(EO$_6$-co-PO$_{29}$) (b) in water at c = 10 g/L versus the temperature.

4. Adsorption isotherms of P(EO-co-PO)-b-PLL copolymers onto model silica nanoparticles

Adsorption isotherms of P(EO-co-PO)-b-PLL copolymers were performed with commercial Ludox TM-50 silica NPs having a diameter of 22 nm according to the manufacturer. Dynamic light scattering performed in 10 mM phosphate buffer pH 7.4 gives a z-average hydrodynamic

diameter of 58 nm and a polydispersity index of 0.20 obtained by fitting the autocorrelation curve with the cumulant algorithm. Ludox particles have a specific surface area of 87 m^2/g according to a previous work (Louguet *et al.* Langmuir 2011, 27, 12891). The same protocol of adsorption as the one described in the experimental section was used with PEO_{113}-*b*-PLL_{10}, $P(EO_{31}$-*co*-$PO_{10})$-*b*-PLL_{13} and $P(EO_6$-*co*-$PO_{29})$-*b*-PLL_{10} copolymers (Figure S6). Isotherms were fitted with the Langmuir equation and results are given in Table S3. Clearly, the molar concentration of adsorbed lysine residues is independent of the type and length of the polyether block, which is a strong evidence of the specific adsorption of PLL blocks onto NPs through electrostatic interactions between positively charged lysine residues and SiO^- groups at silica surface.
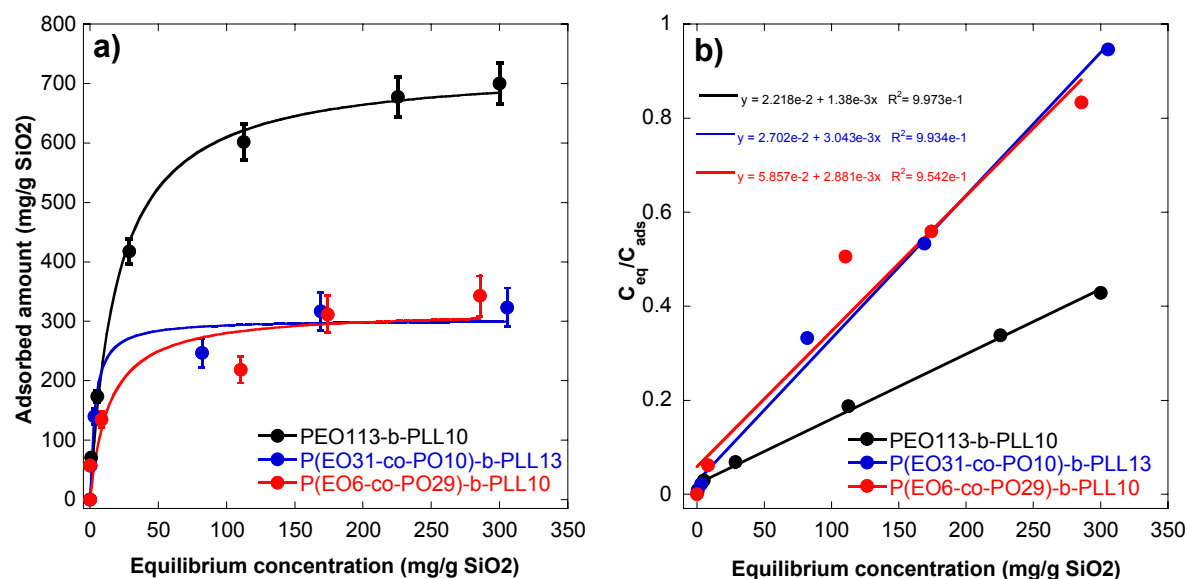
Figure S6. (a) Adsorption isotherms of PEO_{113}-*b*-PLL_{10}, $P(EO_{31}$-*co*-$PO_{10})$-*b*-PLL_{13} and $P(EO_6$-*co*-$PO_{29})$-*b*-PLL_{10} copolymers onto silica nanoparticles in PB (pH 7.4, 10 mM) (b) Langmuir fits.

Table S3. Maximal amounts of PEO_{113}-b-PLL_{10}, $P(EO_{31}$-co-$PO_{10})$-b-PLL_{13} and $P(EO_6$-co-$PO_{29})$-b-PLL_{10} adsorbed on silica particles.

	Maximal adsorbed amount	Maximal adsorbed amount
	mg/g SiO₂	*mmol LL/g SiO₂*
PEO_{113}-b-PLL_{10}	724	1.11
$P(EO_{31}$-co-$PO_{10})$-b-PLL_{13}	328	1.16
$P(EO_6$-co-$PO_{29})$-b-PLL_{10}	347	1.04

The maximal adsorbed amount of PEO_{113}-b-PLL_{10} on ludox NPs is about five times higher than the one found with LSMO@silica MNPs (150 mg copolymer/g particle, see below), which is in good agreement with the difference of specific surface area between ludox silica particles (A = 87 m^2/g) and LSMO@silica MNPs (A= 17 m^2/g; see below).

5. Determination of the surface density of polyether blocks on LSMO@silica MNPs

The data of the adsorption isotherm of PEO_{113}-b-PLL_{10} LSMO@silica MNPs (see Figure 1.a) were fitted by the Langmuir equation:

$$C_{Ads} = \frac{k \times C_{Ads}^{Max} \times C_{eq}}{1 + k \times C_{eq}}$$

where C_{Ads}^{Max} is the maximum mass concentration of surface-adsorbed copolymer chains, C_{eq} is the equilibrium concentration in copolymer and k the adsorption constant ($=k_{adsorption}/k_{desorption}$).

Here, C_{Ads}^{Max} = 0.15 g/g particles and k = 4.3 10^5 L/mol. The specific surface area of LSMO@silica MNPs is given by:

$$S = \frac{3}{d \times r}$$

where r is the radius of particles and d the particle density. The radius is estimated to 27 nm from TEM analysis and the particle density is 6.5 g/cm^3 by neglecting the contribution of the thin silica layer. A specific surface area of 17 m²/g is obtained. The maximal adsorbed amount of copolymer is 8.8 10^{-3} g/m², which corresponds to 0.84 chains per nm² ($M_{copolymer}$ = 6290 g/mol). By considering the total surface of particles as a 2D hexagonal compact lattice, the intermolecular distance D between PEO blocks is given by:

$$D = \frac{2}{(\pi \times \sigma)^{1/2}}$$

where σ is the surface density of PEO blocks. Here, a distance D = 1.2 nm is obtained with σ = 0.84 chains/nm^2.

6. Colloidal stability of PEO-*b*-PLL-modified LSMO@silica MNPs

The stability of NPs coated with PEO$_{113}$-*b*-PLL$_{10}$ was assessed by determining the hydrodynamic sizes of the particles in PB (10 mM, pH 7.4) at various times (Table S4). As seen in Table S4, the hydrodynamic sizes did not significantly change during at least 12 weeks when stored at room temperature, which suggests a high colloidal stability.

Table S4. Hydrodynamic sizes of PEO$_{113}$-*b*-PLL$_{10}$-coated MNPs in PB (pH 7.4, 10 mM) at various times.

Time (day)	D_H (nm)	PDI
0	163	0.12
1	169	0.13
2	168	0.22
4	173	0.25
6	169	0.23
32	174	0.21
72	180	0.16
82	174	0.17

7. Calibration curves of doxorubicin

7.1. Choice of the buffer

The stability of doxorubicin in phosphate buffer (10 mM, pH 7.4) and Tris buffer (25 mM, pH 7.4) was studied by determining the optical density before and after centrifugation of doxorubicin solutions varying in concentration (Table S5). The same conditions of centrifugation as those used for the centrifugation of MNPs coated with copolymer were chosen.

Table S5. Optical density ($\lambda = 485$ nm) of doxorubicin solutions in PB (10 mM, pH 7.4) and in Tris (25 mM, pH 7.4) before and after centrifugation (11092 g, 30 min, 10°C)

C_{DOX} (µg/mL)	PB (7.4, 10 mM)		Tris (7.4, 25 mM)	
	Initial	*Centrifuged*	*Initial*	*Centrifuged*
116	0.535	0.5	0.953	0.957
232	1.698	1.54	1.809	1.804
500	2.995	1.898	3.375	3.37

Clearly, doxorubicin molecules have a strong tendency to aggregate in phosphate buffer as seen by the decrease in optical density of doxorubicin solutions after centrifugation. It is supposed that divalent salts in PB interact with the positively charged amino groups of doxorubicin leading to the precipitation of the drug molecules. Similar experiments performed in water with NaCl showed no aggregation upon centrifugation.
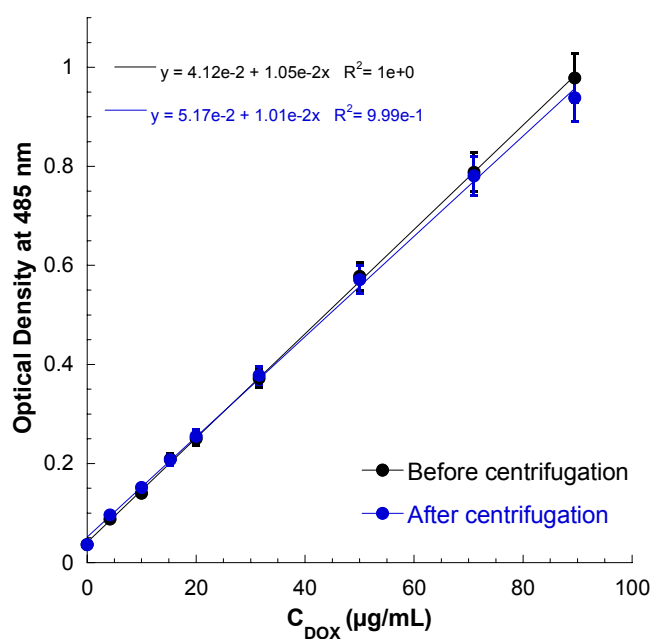
7.2. Doxorubicin titration

Because doxorubicin is known for undergoing degradation in aqueous solutions, the absorbance of doxorubicin solutions in Tris buffer (25 mM, pH 7.4) varying in concentration was monitored over time (Figure S7). A slight decrease in absorbance was observed over time and was taken into account for calculations of loading contents and loading efficiencies of doxorubicin in MNPs.
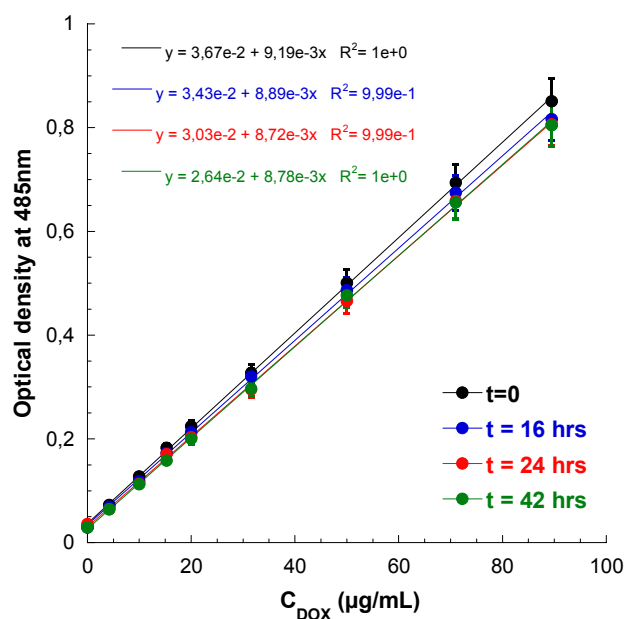

Figure S7. Optical density of doxorubicin solutions in Tris buffer (25 mM, pH 7.4) over time.

Incubation of doxorubicin with copolymer-modified MNPs was conducted at room temperature and at 50°C. In order to verify the influence of the temperature on doxorubicin stability, solutions of doxorubicin were heated at 50°C for 8 h and centrifuged (11092 g, 30 min, 10°C). Optical density of the initial solutions as well as the supernatants was measured. As seen in Figure S8, no aggregation occurs upon heating and centrifugation steps.

Figure S8. Optical density of doxorubicin solutions in Tris buffer (25 mM, pH 7.4) at various concentrations after incubation at 50°C for 8 hrs before and after centrifugation (11092 g, 30 min, 10°C).

For drug release experiments, doxorubicin was titrated by fluorescence spectroscopy (λ_{ex} = 485 nm, λ_{em} = 590 nm) to have a high sensitivity. Calibration curves of doxorubicin solutions at 25 °C and 43 °C are shown in Figure S9. The fluorescence intensity slightly decreases with time as previously observed with absorbance measurements. No significant differences are observed when comparing fluorescence intensities of doxorubicin solutions incubated 8 h at 25 °C or at 43 °C.
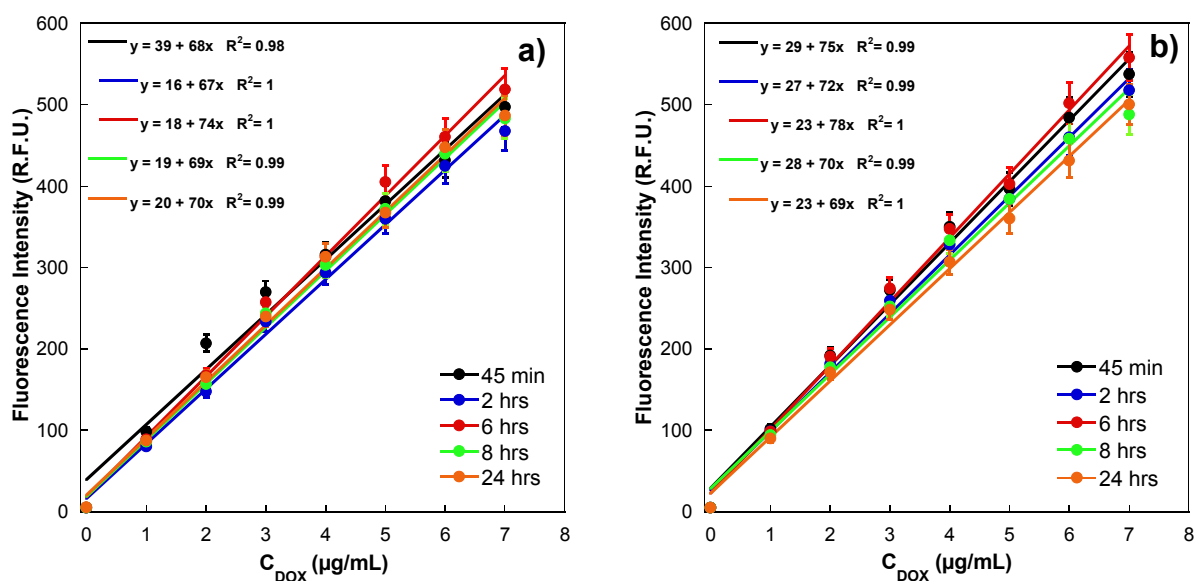
Figure S9. Fluorescence intensity of doxorubicin in Tris buffer (25 mM, pH 7.4) at various concentrations and incubation times at 25 °C (a) and 43 °C (b).

## 8. Synthesis of fluorescein-labeled PEO-*b*-PLL copolymer

α,ω-amino, trityl-protected sulfhydril-PEO$_{113}$ was used to initiate the ring-opening polymerization of TFA L-lys NCA in similar conditions as those used for the synthesis of the PEO$_{113}$-*b*-PLL$_{10}$ copolymer (see experimental section) (Figure S10). After deprotection of TFA L-lys units with KOH in THF, the trityl protecting group was removed by acid hydrolysis in presence of a reductive agent. Then, the thiol group was modified with fluorescein 5-maleimide using a labeling kit from Pierce.
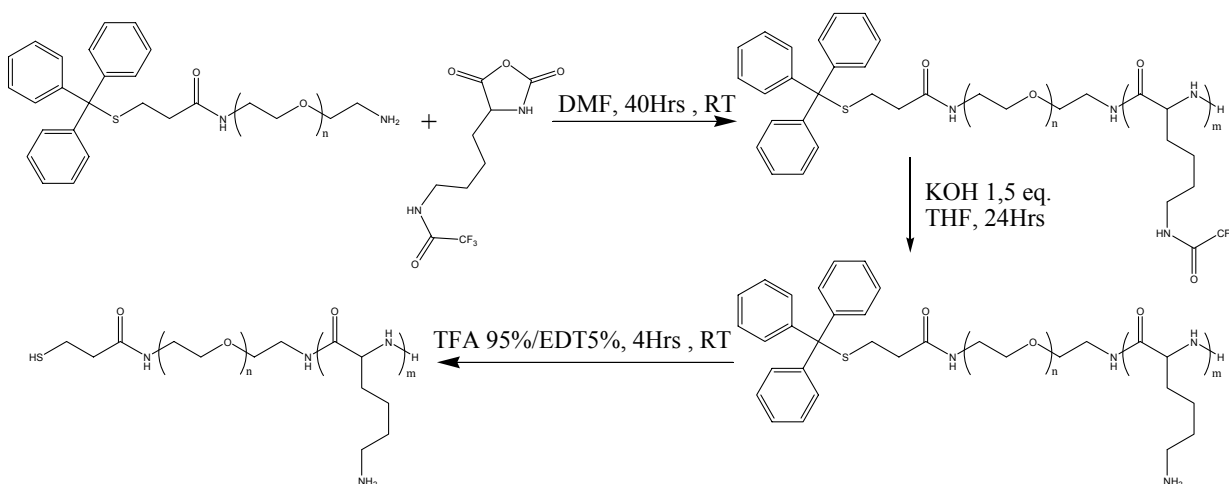
Figure S10. Synthesis of HS-PEO-*b*-PLL copolymer from a bifunctional macroiniator.

9. Experimental setup for studying the drug release under various conditions

A dialysis bag containing 2.5 mL of copolymer-modified MNPs dispersion loaded with doxorubicin was placed into a measuring cylinder filled with 100 mL of Tris buffer (25 mM, pH 7.4) under stirring. The release at 25 °C was performed in an air-conditioned room (Figure S11.a). For the release conducted at 43°C, the whole assembly was placed in an oil bath (Figure S11.b) on a heating plate. For the release experiment performed in the presence of an alternating magnetic field, the cylinder was placed in the center of a coil connected to a generator (Figure S11.c).
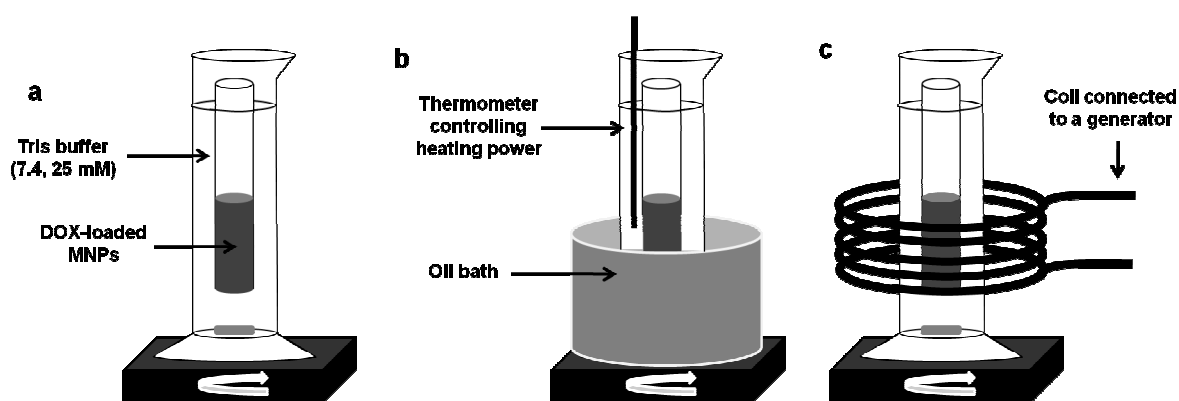
Figure S11. Setups for monitoring the release of doxorubicin from copolymer-modified MNPs at 25 °C (a), at 43 °C (b) and at 25 °C by applying AMF (c).